Earth and Planetary Science Letters 305 (2011) 283–289

Contents lists available at ScienceDirect

Earth and Planetary Science Letters

journal homepage: www.elsevier.com/locate/epsl

# Dynamics of stick–slip motion, Whillans Ice Stream, Antarctica

J. Paul Winberry [a,*], Sridhar Anandakrishnan [b], Douglas A. Wiens [c], Richard B. Alley [b], Knut Christianson [b]

[a] Department of Geological Sciences, Central Washington University, Ellensburg, WA 98926, USA
[b] Department of Geosciences, The Pennsylvania State University, University Park, PA 16802, USA
[c] Department of Earth and Planetary Sciences, Washington University, St Louis, MO 63130, USA

ARTICLE INFO

*Article history:*
Received 28 November 2010
Received in revised form 24 February 2011
Accepted 26 February 2011
Available online 6 April 2011

Editor: P. Shearer

*Keywords:*
glacial geophysics
ice stream
seismology

ABSTRACT

The stick–slip motion and associated seismic emissions of Whillans Ice Stream (WIS), West Antarctica are two of the many recent observations of unexpected ice sheet behavior that are challenging traditional models of rapid glacier motion. Here we find that the WIS slip events repeatedly nucleate from a sticky-spot located in the middle of the ice stream, acting similar to an asperity in traditional models of earthquake physics. This region shows less motion than surrounding areas during the inter-slip periods, thus, concentrating stress and producing a pulse of seismic energy at the onset of slip. The propagating rupture breaks through an additional asperity in the northern part of the ice stream, producing another pulse of seismic energy 6–12 min after initiation. Both asperities are regions of higher hydraulic potential than surrounding regions, suggesting they may have greater bed friction due to reduced water lubrication. Tidal pacing of the stress accumulation combined with fault healing controls the applied stress at failure, with higher stress giving faster propagation of the rupture front and higher slip velocities; these differences are reflected in the timing of the teleseismic arrivals. Our results highlight both the great sensitivity of large ice streams to small changes in external forcing and the importance of limited regions of the subglacial bed in controlling their motion, as well as providing insights to the mechanics of repeating earthquakes.



## 1. Introduction

Ice streams are the primary routes for ice to be discharged from the Earth's ice sheets, thus understanding the physical basis for their rapid motion will help in the understanding of both future and past ice sheet evolution (Bentley, 1987). Recent observations have shown that much of the downstream portion of the Whillans Ice Stream (WIS), West Antarctica, remains virtually stagnant during most of the day except for two short bursts (≈20 min each) of motion during each of which the ice stream moves forward by ≈0.4 m (Bindschadler et al., 2003). The regular occurrence of two slip events per day arguably makes WIS the most predictable large-scale stick–slip system in nature. During the "stick" portion of a cycle, basal-shear stress increases in the stick–slip region as it is loaded elastically by flow in continuously slipping regions upglacier and downglacier. The motion during the "slip" phase releases the stored elastic strain, in a cycle similar to the tectonic loading and seismic failure of faults. Thus, understanding the dynamics of WIS will not only improve our understanding of ice sheet dynamics, but will potentially shed light on the fundamental processes of unstable slip (Peng and Gomberg, 2010). Wiens et al. (2008) showed that these WIS slip events also generate seismic energy that can be detected at far-field (>900 km) seismic stations. In this manuscript, we examine the spatial and temporal behavior of the WIS stick–slip cycle and how the tidal modulation of subglacial stress influences the dynamic behavior of the ice stream and associated seismic emissions.

## 2. Geodetic observations

We investigate the dynamics of the WIS stick–slip cycle using a network of 20 high-rate (0.1 Hz) GPS sites deployed on the WIS during the 2004–2005 austral summers (Fig. 1). GPS antennas were affixed to metal poles, and stations were powered by a combination of batteries and solar panels. Sites were analyzed using the Track software to solve for three-dimensional WIS site coordinates at the full data rate of 0.1 Hz (Chen, 1998). Site motion was loosely constrained at 0.05 m every 10 s, which reduces noise without over-smoothing the signal. The precision of the coordinates was assessed during WIS inter-slip time periods or at linearly moving sites, and is ≈0.01 m and ≈0.03 m in the horizontal and vertical coordinates, respectively. Fig. 2 shows raw displacement time-series for a single slip event.

Tidally paced variations in the subglacial stress cause one of the two daily slip events to occur near the daily low tide, with the other near the daily high tide (tides in this region are primarily diurnal rather than semidiurnal)(Bindschadler et al., 2003). Although some modulation is observed in association with spring–neap tidal cycling, successive high-tide events are quite similar, as are successive low-

* Corresponding author. Tel.: +1 509 899 2716.
*E-mail address:* winberry@geology.cwu.edu (J.P. Winberry).

0012-821X/$ – see front matter © 2011 Elsevier B.V. All rights reserved.
doi:10.1016/j.epsl.2011.02.052

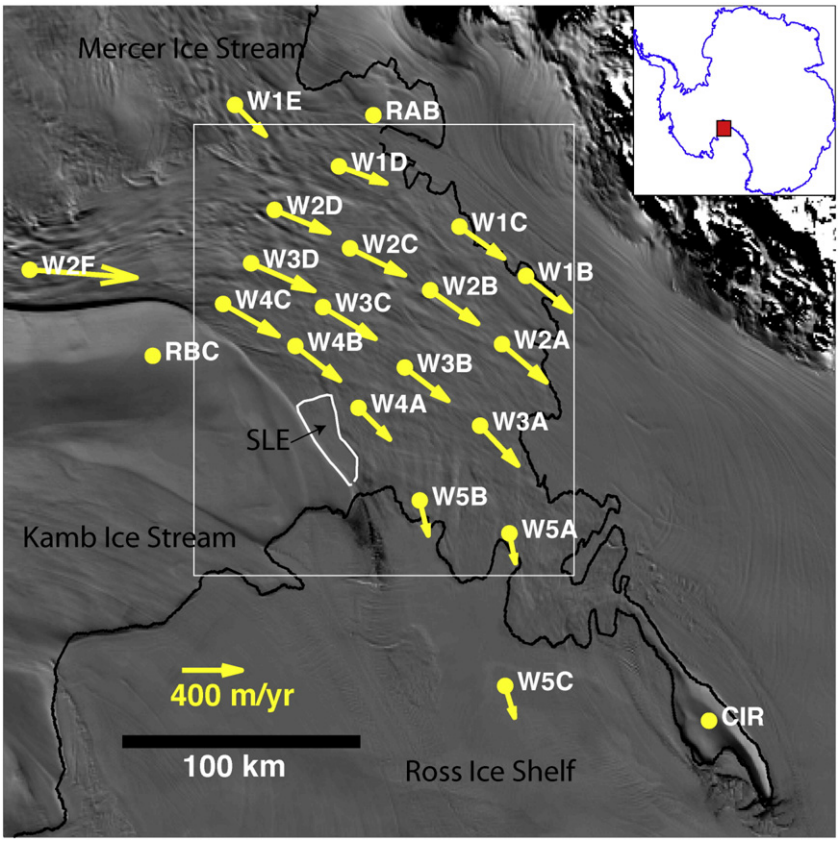


**Fig. 1.** Study area. Black line is grounding line. Location and annual average velocity vectors are plotted. White box outlines the region shown in Figs. 4 and 5. Black line is the grounding line (Horgan and Anandakrishnan, 2006). Subglacial Lake Engelhardt (SLE) is highlighted. Background image is from the MODIS Mosaic of Antarctica (Haran et al., 2005).

tide events. We thus choose to focus here on one high-tide and one low-tide event in a single day during the peak of the spring–neap tide cycle, to avoid loss of resolution that might result from averaging across multiple events.

## 3. Inter-event motion and subglacial sticky-spots

Wiens et al. (2008) proposed that a large subglacial sticky-spot at the center of the ice stream, near station W2B, makes a disproportionate contribution to overall basal drag of the ice stream between slip events, acting as an asperity as treated in traditional models of earthquake physics. The theory was based on the observation that all slip events appear to repeatedly nucleate from a single location near station W2B (Fig. 2). We hypothesize that regions in and near sticky-spots should show relatively small displacements during inter-event periods, similar to the behavior of earthquake faults.

We investigate this hypothesis by mapping the motion of the ice stream both before and during a low-tide event and the following high-tide event (Fig. 3). The onset and termination of slip events have been picked manually and the results have been interpolated onto a 10 km grid using a linear interpolation. The first-order displacement patterns are similar for the two inter-event periods, and for the two slip events. During inter-event periods, two regions of relatively small-motion are observed (sticky spots or asperities): one near the center of ice stream (station W2B), and a second near the grounding line between stations W5B and W5A. Regions surrounding the sticky spots show more motion between slip events, of up to 1 m/day. During slip events, displacement is largest near the center of the ice stream, tapering upstream and towards the margins, but accounts for the deferred displacement over the sticky spots that result from low inter-event motion so that the total displacement over a tidal cycle is the same. Earlier studies of displacement in the region (Bindschadler et al., 1987) would not have observed these patterns due to the fact that when integrated over longer time-scales (a few days) the characteristic displacement field observed for each period of the stick–slip cycle produce a typical ice stream cross-sectional displacement profile.

Sticky spots or asperities, such as those suggested by our maps of inter-event displacement, may have many causes (Alley, 1993). Whillans Ice Stream is known to have extensive, soft subglacial till, the fault gouge of this system (Blankenship et al., 1987; Kamb, 2001). The simplest hypothesis for the cause of sticky spots is till discontinuity around a resistant bedrock high. However, given the sensitivity of till properties to water pressure (Tulaczyk et al., 2000), sticky spots may arise from locally insufficient basal water to maintain low effective normal pressure required for stable sliding. We investigated this hypothesis by constructing a map of subglacial hydraulic potential pressure for WIS using a new 1 km surface DEM (Bamber et al., 2009) and original bed topography from 1980s airborne radar surveys (Shabtaie et al., 1988). Water under ice sheets moves opposite to the negative gradient of static hydraulic potential pressure. We calculate static hydraulic potential pressure ($\Phi$) underneath Whillans Ice Stream:

$$\Phi = \rho_i g z_s - (\rho_w - \rho_i) g z_b \quad (1)$$

where $\rho_i$ and $\rho_w$ are the density of ice and water, respectively, and $z_s$ and $z_b$ are the surface and bed elevation, respectively (Shreve, 1972). All data was interpolated to 1 km (the resolution of the surface DEM) using continuous curvature splines in tension (Smith and Wessel, 1990). Due to navigation inaccuracies along flight lines of the radar survey, in places exceeding 1 km, this map of static hydraulic potential pressure should be treated as approximate and used only to interpret general trends in water flow.

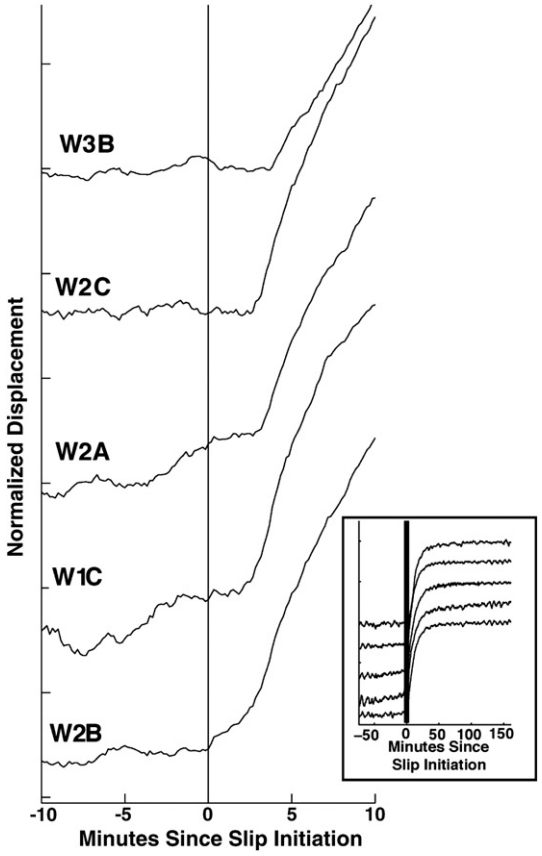


**Fig. 2.** Displacement time series for a twenty-minute window around the onset of a slip event. Note that Rupture is first observed W2B in the middle of the ice stream. The inset shows an expanded time window of the same slip event. The data have been normalized by dividing each time series by the maximum displacement for each record during the plotted time period.

Both sticky-spots inferred from our maps of inter-event displacement coincide with ridges in $\Phi$. The proposed nucleation sticky-spot is surrounded by two valleys in HP that will tend to divert water away from the region and towards the grounding line (Fig. 4). An ongoing geophysical field program is aimed at more precisely locating this sticky-spot, its bed elevation signature, and determining its physical properties (i.e., till versus bedrock). The downstream sticky-spot is located downstream of a large ridge in the HP map, with water diverted into subglacial lakes that form in $\Phi$ basins (Fricker and Scambos, 2009)(Fig. 4). For the downstream sticky-spot and lake, these results suggest that the lakes may be sequestering water at the expense of the surrounding ice stream, with the lake filling before an outburst flood (Winberry et al., 2009a). These results highlight the important connections between the subglacial water-system and the stability of ice streams, including the ongoing deceleration of the entire WIS. For example, the region around the downstream sticky-spot is presently experiencing the highest rate of deceleration on the ice stream (~1.5% annually (Joughin et al., 2005)), suggesting that the formation of the downstream sticky-spot and the onset of stick–slip behavior may be playing a significant role in the present deceleration (Sergienko et al., 2009) and century-scale fluctuations of WIS (Hulbe and Fahnestock, 2004).

## 4. Inter-event slip and tidal pacing of Whillans Ice Stream motion

Our observations of inter-event motion confirm the tidal pacing of the WIS stick–slip cycle, building upon previous work that relied on tidal models to infer the tidal modulation of basal shear stress (Bindschadler et al., 2003; Winberry et al., 2009b). For example, upstream station W3C moves at a relatively steady rate during inter-event periods, 0.96 m/day prior to the low tide event and 0.90 m/day prior to the high tide event. In contrast, downstream station W2A moves over three times faster before the low tide event than before the high tide event (0.15 m/day versus 0.5 m/day) (Fig. 3). This tidal modulation of flow between slip events at downstream sites is consistent to observation of tidal modulated flow on other Antarctic ice streams (Anandakrishnan et al., 2003; Gudmundsson, 2007; Murray et al., 2007).

The analysis of inter-event motion indicates that a large asperity near the center of WIP is the locus of resistance. The spatial resolution of the current data set is too coarse to resolve stress and identify the precise location of the asperity, thus we use a modified version of equation 1 from Bindschadler et al. (2003) to estimate the first order relative contributions of the upstream and downstream components to the basal shear stress budget on the nucleation sticky-spot. We average over the length of the ice plain while we await the collection of higher-resolution geodetic observations from future field studies. For the purposes of this paper, we restrict ourselves to two station pairs: (1) W3D–W2B to estimate basal shear stress $\tau_{upstream}$ that results from upstream compression; and (2) W2B–W2A to estimate basal shear stress $\tau_{downstream}$ that result from downstream extension. The average basal shear stress between two points is estimated by

$$\tau = E\frac{x}{L^2}H \tag{2}$$

where $E$ is shear modulus of ice (~$10^{10}$ Pa), $x$ is the change in difference in inter-event motion between the two stations, $L$ (76 km for W3D–W2B and 37 km for W2B–W2A) is the original distance between two stations, and $H$ is the average ice thickness (~800 m). For the low-tide event, $\tau_{upstream} = 0.3$ kPa and $\tau_{downstream} = 0.68$ kPa while for the high-tide event, $\tau_{upstream} = 0.63$ kPa and $\tau_{downstream} = 0.20$. The average basal shear over the entire WIP is then estimated by

$$\tau_{avg} = \tau_{upstream}\left(\frac{L_{upstream}}{L_{upstream} + L_{\text{downstream}}}\right) + \tau_{downstream}\left(\frac{L_{downstream}}{L_{upstream} + L_{downstream}}\right) \tag{3}$$

Using these we values find the average basal shear stress of 0.42 kPa prior to the initiation of the low-tide event and 0.49 kPa for the high-tide event.

The increased flow rate near station W2A during the falling tide results in a near doubling of the rate at which stress is applied to the bed of the ice stream (~0.07 kPa/h versus ~0.03 kPa/h), causing the yield strength of the bed to be reached earlier. This tidal pacing is accentuated by the time-dependent yield strength of the ice-stream bed (Winberry et al., 2009b), which slowly strengthens after the termination of a slip event. As a consequence of this tidal modulation, the low-tide event initiates at a lower stress level (~0.42 kPa versus ~0.49 kPa) and after less accumulation of elastic deformation, resulting in less displacement during the slip event. It is worth noting that these values are low compared to many other ice streams, where basal drag often exceeds 20 kPa (Joughin et al., 2004; Joughin et al., 2006). The low surface slopes and resulting small driving stresses on the downstream portion of WIS produce a system sensitive to relatively small perturbations.

## 5. Rupture dynamics and far-field seismic radiation

Wiens et al. (2008) showed that the rapid motion during slip events generates seismic energy that can be recorded at great distances (>500 km), prompting us to investigate the evolution of slip velocity during each slip event to help elucidate the origins of these arrivals and their relation to WIS motion (Fig. 5). To produce the velocity time-series we apply a 600 second low pass filter prior to

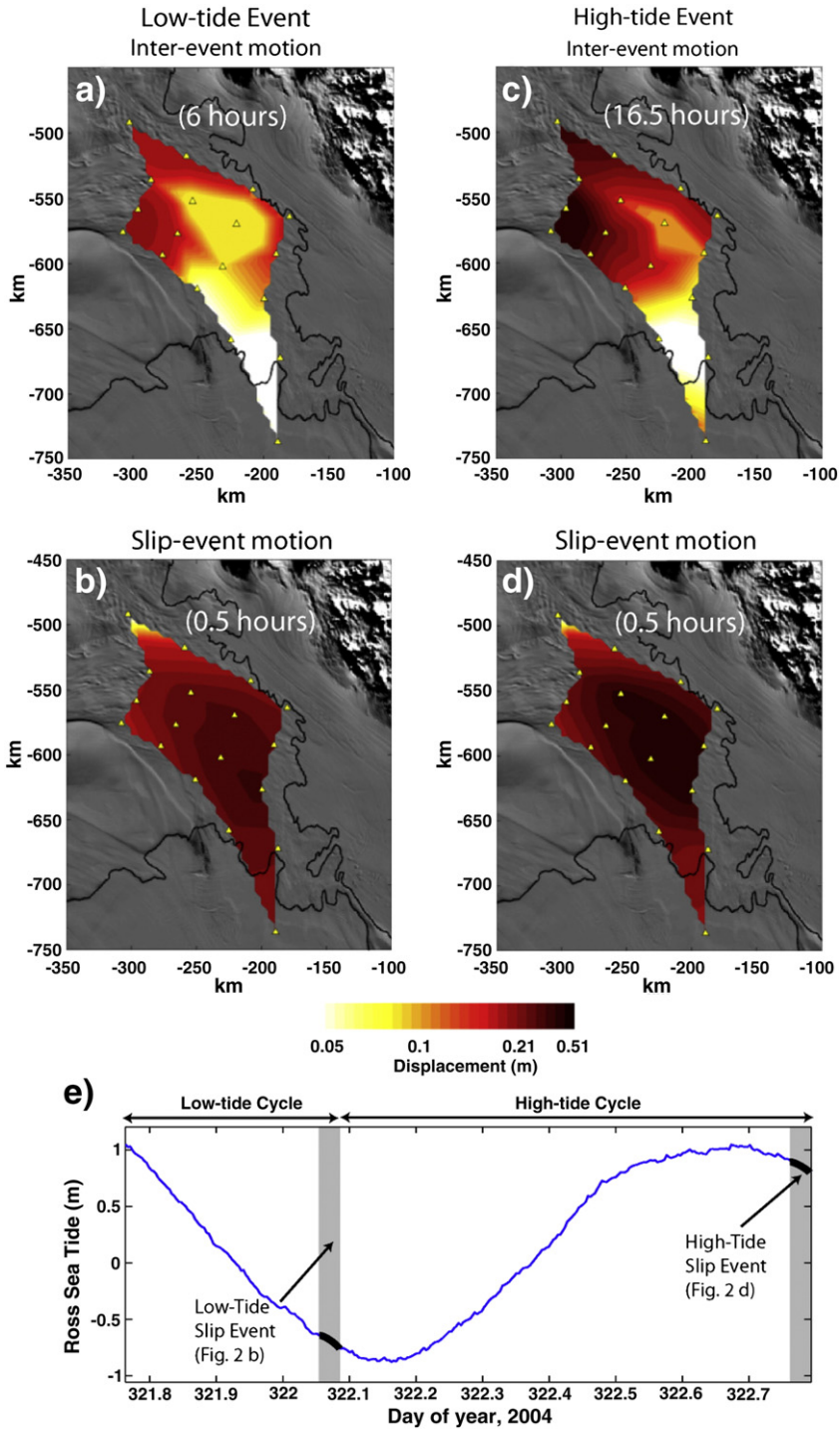


**Fig. 3.** Panels a and c, show the total displacement during the inter-event preceding each two slip events. Panels b and d, show the total motion during each slip event. Note the non-linear color scale. Panel e shows the tides of the Ross during these two stick–slip cycles as measured by the vertical component of motion at W5C.

differentiating the displacement time-series. A cubic interpolation was used to map displacement and velocity for the entire ice plain at each sampling interval. Due to noise in the velocity data, we only show data when slip velocity exceeds 10 m/day. The GPS observations of slip velocity were also used to calculate the moment-rate-function (MRF) for each slip event (Fig. 6) (Lay and Wallace, 1995). The MRF is derived using the expression

$$\mathrm{MRF}(t) = \mu \mathrm{AD} \tag{4}$$

where $\mu$ is the shear modulus of ice ($\sim 10^{10}$ Pa), A is the area of the slipping region ($\sim$15,000 km$^2$), and D is the average displacement during the time step. The MRF is commonly used to study the dynamic behavior of earthquakes as it represents the total forcing available for producing seismic waves. Thus, the MRF complements the snapshots of slip velocity by providing a spatially integrated time-series of slip behavior that can be more easily compared with seismograms.

Both slip events initiate near the central sticky-spot of the ice stream (station W2B) and propagate outward, with the rupture front expanding about twice as rapidly upglacier and downglacier as it does

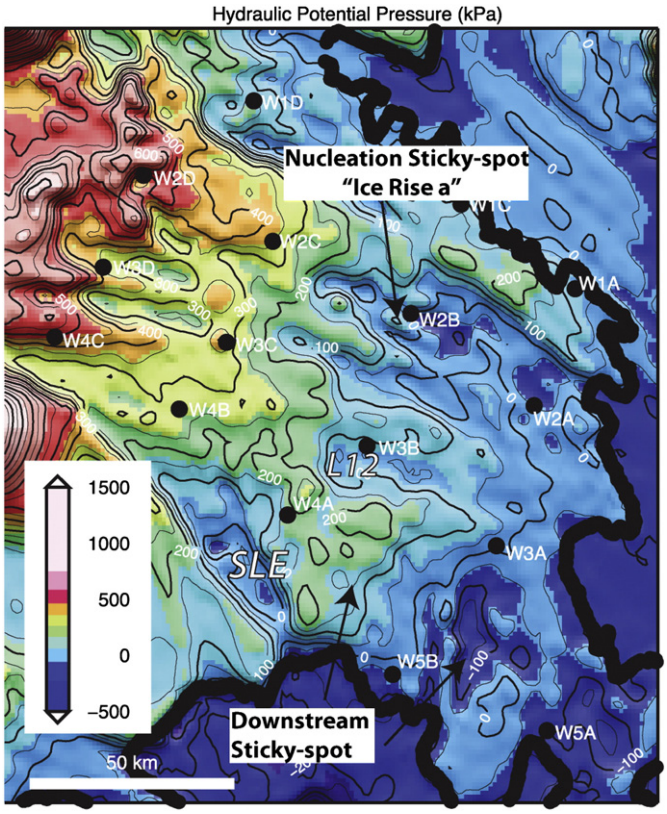


**Fig. 4.** Subglacial Hydraulic Potential for study area. Note the ridge in to the north of W2B that appears to be the region of slip event nucleation. In addition, a large ridge exist between, W4A and W5B, the location of the second sticky-spot. Subglacial Lake Engelhardt (SLE) and Lake 12 from Fricker and Scambos (2009) are labeled.

transverse to ice flow (Fig. 5). For example, during the high-tide event rapid motion begins at station W2D at ~75 km distance along flow within 200 s (~375 m/s) while slip does not begin at station W4A at ~58 km distance across flow until 335 s (~170 m/s). The spacing of our sensors is sufficiently large to allow for spatial aliasing, but the slip appears to propagate especially rapidly downglacier and then across Subglacial Lake Engelhardt, slow in the vicinity of the grounding-line sticky spot, and then accelerate onto the ice shelf after breaking through this second sticky spot.

The primary differences between the high-tide and low-tide event are: (1) the rupture propagates more slowly in the low-tide event than in the higher-stress high-tide event (for example, slip begins over 4 min later at W4A in the low-tide event—11 min versus 5.6 min—indicating a ~50% reduction in rupture speed); and (2) peak slip velocities are typically lower during the low-tide event. The most striking manifestation of the slower rupture propagation in the low-tide event is the three-minute delay in the secondary velocity peak across Subglacial Lake Engelhardt and surroundings (~14 min in the low-tide event, compared to ~11 min for the high tide event). The longer delay in the low-tide event allows greater time separation between triggering of the event and propagation across the lake, causing the MRF for the low-tide event to have a much more prominent double peaked character. The lower rupture velocity and slip velocity in the low-tide event both likely arise from the smaller stress reduction in the low-tide event, which in turn results from the greater rate of stress accumulation and thus less time for fault healing in the low-tide event (Winberry et al., 2009b).

The variation in dynamic behavior between the two slip-events is reflected in the timing of seismic arrivals of the event recorded at South Pole (Fig. 6). The slip events generate three packets of seismic energy observable on the horizontal component of motion at South Pole. Wiens et al. (2008) showed that the first seismic arrival (plotted as ~0 min for each event) is generated by the rapid transition from slow to fast motion at the beginning of a slip event, but the origins of the second and third arrivals were less clear.

Our results show that the second arrival corresponds to the secondary geodetically imaged speed-up while the third appears to occur with the reduction in MRF and may represent a stopping phase. The shorter times between the arrivals for the high-tide event are consistent with the faster rupture propagation imaged by GPS in response to the larger accumulated stress. Ideally the seismic amplitudes could be directly related to the MRF however, the observed waveforms are generated by the short-period (<200 s) component of the MRF that is difficult to directly observe due to noise in the GPS motion data at these periods.

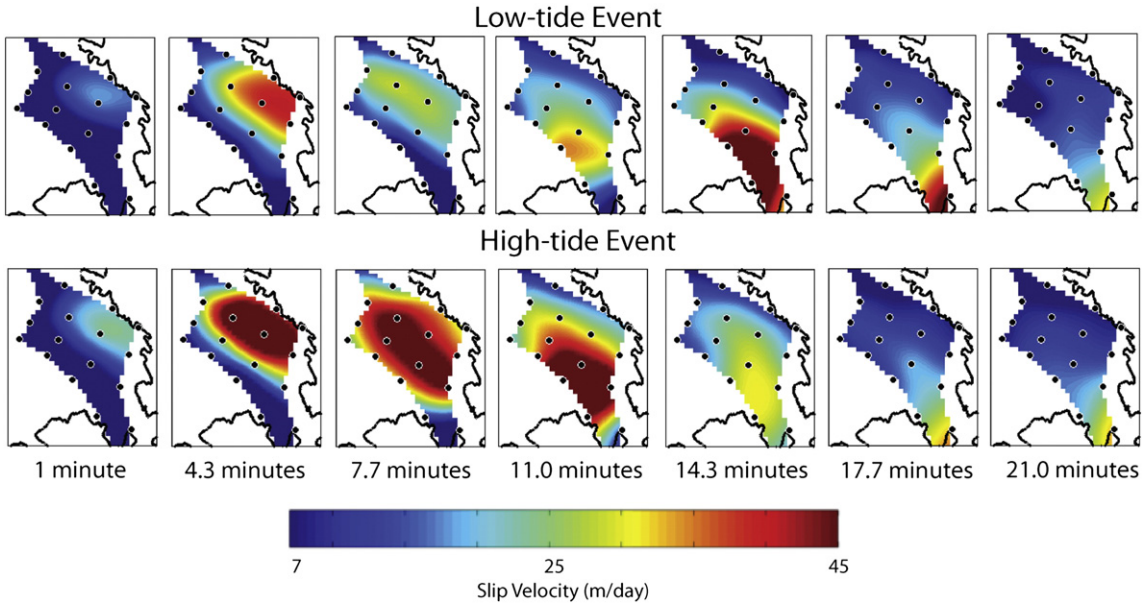


**Fig. 5.** Evolution of slip and slip velocity for the two slip events. Each event is characterized by a migration of peak slip velocities from the center of the ice stream towards the northern grounding line. Faster rupture propagation results in this secondary speed-up occurring earlier during the high-tide event (~11 min versus ~14 min). Black dots show GPS locations.

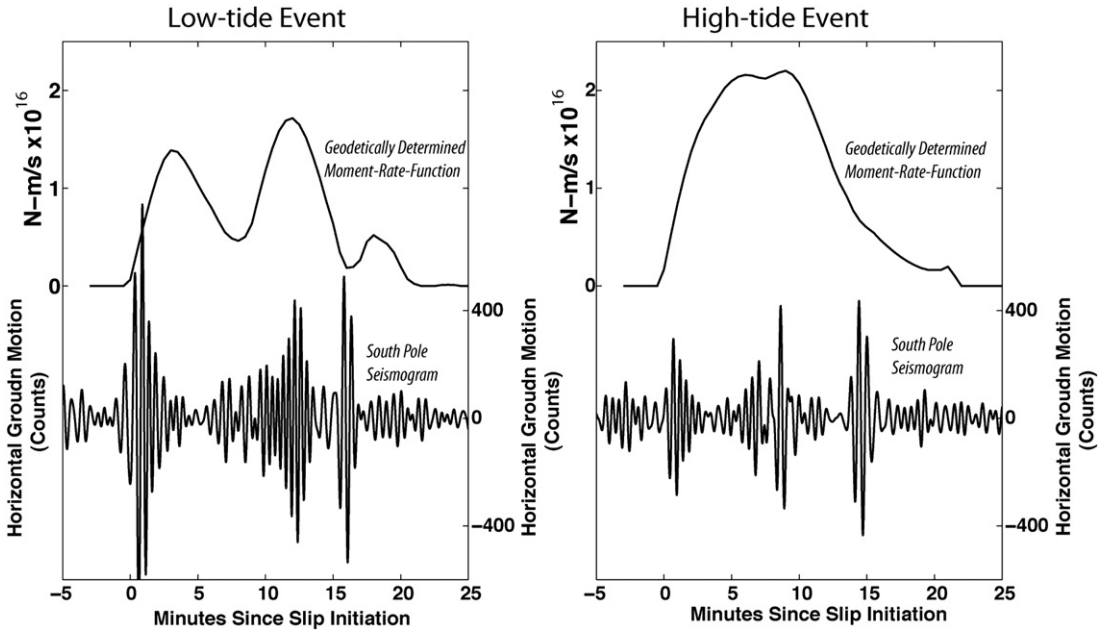


**Fig. 6.** Moment-rate-functions and seismograms observed at South Pole for the two events. The waveforms have been shifted in time to account for the approximate travel time between WIS and South Pole and each has been band-passed filtered at 0.02–0.04 Hz.

## 6. Summary

Our results highlight the spatial and temporal complexity of this dynamic form of motion and provide an observational and theoretical basis for future research. The rapid accelerations on WIS and the discovery of large "glacial earthquakes" near several large outlet glaciers of the Greenland Ice Sheet (Ekström et al., 2003) suggest that short-term fluctuations in glacier behavior that can produce teleseismic emissions are ubiquitous features of ice sheet flow. However, the study of their dynamics and the role of these short-term fluctuations in the long-term stability of ice sheets remain in its infancy (Gudmundsson, 2007; Tulaczyk, 2006; Winberry et al., 2009b). Future studies that address these short-term fluctuations have the potential to provide insight into the underlying mechanisms of fast glacier motion. Glaciologically, our results show the existence of "sticky spots" likely related to reduced subglacial lubrication and strongly affecting ice motion, providing targets for field research aimed at understanding controls on ice-stream motion and stability. Seismologically, the stick–slip dynamic behavior of WIS provides a potential analogue for understanding stick–slip processes in general. While different from tectonic faults, the predictable timing of the slip events on WIS makes them a great target for understanding unstable sliding in nature, in particular the interactions between spatial heterogeneities in friction along the sliding interface and rupture dynamics. We find inter-event time strengthening, asperity triggering, faster propagation along flow than across, faster propagation and faster slip with higher accumulated stress, variations in propagation velocity in response to spatial heterogeneity of the fault plane, delay and breakthrough at a second asperity, and extensive generation of seismic energy from the onset and cessation of motion as well as from variations during propagation.

## Acknowledgements

This work was supported the US-NSF foundation grants 0229629 and 0424589. M.A. King processed the GPS data. We thank members of the TIDES team for help with the field program. Seismic data was obtained from the IRIS data center. GPS instrumentation was supplied by the UNAVCO. Logistical support was provided Raytheon Polar Services, New York Air National Guard, and Ken Borek Air.

## References

Alley, R., 1993. In search of ice stream sticky spots. J. Glaciol. 39, 447–454.
Anandakrishnan, S., Voigt, D.E., Alley, R.B., King, M.A., 2003. Ice stream D flow speed is strongly modulated by the tide beneath the Ross Ice Shelf. Geophys. Res. Lett. 30 (7), 1361. doi:10.1029/2002GL016329.
Bamber, J., Gomez-Dans, J., Griggs, J., 2009. A new 1 km digital elevation model of the Antarctic derived from combined satellite radar and laser data — Part 1: data and methods. Cryosphere 3, 101–111.
Bentley, C.R., 1987. Antarctic ice streams—a review. J. Geophys. Res. 92, 8843–8858.
Bindschadler, R.A., Stephenson, S.N., Macayeal, D.R., Shabtaie, S., 1987. Ice dynamics at the mouth of Ice Stream-B, Antarctica. J. Geophys. Res. Solid Earth Planets 92, 8885–8894.
Bindschadler, R.A., King, M.A., Alley, R.B., Anandakrishnan, S., Padman, L., 2003. Tidally controlled stick–slip discharge of a West Antarctic ice stream. Science 301, 1087–1089.
Blankenship, D.D., Bentley, C.R., Rooney, S.T., Alley, R.B., 1987. Till beneath Ice Stream-B. 1. Properties derived from seismic travel-times. J. Geophys. Res. Solid Earth Planets 92, 8903–8911.
Chen, G., 1998. GPS Kinematics Positioning for the Airborne Laser Altimetry at Long Valley. Massachusetts Institute of Technology, California.
Ekström, G., Nettles, M., Abers, G., 2003. Glacial earthquakes. Science 302, 622–624.
Fricker, H.A., Scambos, T., 2009. Connected subglacial lake activity on lower Mercer and Whillans Ice Streams, West Antarctica, 2003–2008. J. Glaciol. 55, 303–315.
Gudmundsson, G.H., 2007. Tides and the flow of Rutford Ice Stream, West Antarctica. J. Geophys. Res. Earth Surf. 112.
Haran, T., Bohlander, J., Scambos, T., 2005. MODIS mosaic of Antarctica (MOA) image map, National Snow and Ice Data Center.
Horgan, H., Anandakrishnan, S., 2006. Static grounding lines and dynamic ice streams: evidence from the Siple Coast, West Antarctica. Geophys. Res. Lett. 33.
Hulbe, C.L., Fahnestock, M.A., 2004. West Antarctic ice-stream discharge variability: mechanism, controls and pattern of grounding-line retreat. J. Glaciol. 50, 471–484.
Joughin, I., MacAyeal, D.R., Tulaczyk, S., 2004. Basal shear stress of the Ross Ice Streams from control method inversions. J. Geophys. Res. Solid Earth 109.
Joughin, I., Bindschadler, R., King, M., Voigt, D., Alley, R., Anandakrishnan, S., et al., 2005. Continued deceleration of Whillans Ice Stream, West Antarctica. Geophys. Res. Lett. 32.
Joughin, I., Bamber, J.L., Scambos, T., Tulaczyk, S., Fahnestock, M., MacAyeal, D.R., 2006. Integrating satellite observations with modelling: basal shear stress of the Filcher-Ronne ice streams, Antarctica. Philos. Trans. A Math. Phys. Eng. Sci. 364, 1795–1814.
Kamb, B., 2001. Basal zone of the West Antarctic ice streams and its role in lubrication of their rapid motion. In: Alley, R.B., Bindschadler, R.A. (Eds.), The West Antarctic Ice Sheet: Behavior and Environment, AGU.
Lay, T., Wallace, T., 1995. Modern Global Seismology. Academic Press.
Murray, T., Smith, A.M., King, M.A., Weedon, G.P., 2007. Ice flow modulated by tides at up to annual periods at Rutford Ice Stream, West Antarctica. Geophys. Res. Lett. 34.
Peng, Z., Gomberg, J., 2010. An integrated perspective of the continuum between earthquakes and slow-slip phenomena. Nat. Geosci. 3, 599–607.
Sergienko, O., Macayeal, D., Bindschadler, R., 2009. Stick–slip behavior of ice streams: modeling investigations. Ann. Glaciol. 50, 87–94.
Shabtaie, S., Bentley, C.R., 1988. Ice-thickness map of West Antarctic ice streams by radar sounding., Ann. Glaciol. 11, 126–136.

Shreve, R., 1972. Movement of water in glaciers. J. Glaciol. 11, 205–214.
Smith, W., Wessel, P., 1990. Gridding with continuous curvature splines in tensions. Geophysics 55, 293–305.
Tulaczyk, S., 2006. Scale independence of till rheology. J. Glaciol. 178, 377–380.
Tulaczyk, S., Kamb, W.B., Engelhardt, H.F., 2000. Basal mechanics of Ice Stream B, West Antarctica 2. Undrained plastic bed model. J. Geophys. Res. Solid Earth 105, 483–494.
Wiens, D.A., Anandakrishnan, S., Winberry, J.P., King, M.A., 2008. Simultaneous teleseismic and geodetic observations of the stick–slip motion of an Antarctic ice stream. Nature 453, 770–774.
Winberry, J.P., Anandakrishnan, S., Alley, R.B., 2009a. Seismic observations of transient subglacial water-flow beneath MacAyeal Ice Stream, West Antarctica. Geophys. Res. Lett. 36.
Winberry, J.P., Anandakrishnan, S., Alley, R.B., Bindschadler, R.A., King, M.A., 2009b. Basal mechanics of ice streams: insights from the stick–slip motion of Whillans Ice Stream, West Antarctica. J. Geophys. Res. Earth Surf.